Transitions across a barrier induced by deterministic forcings

C. Nicolis
Institut Royal Météorologique de Belgique, Avenue Circulaire 3, 1180 Brussels, Belgium

G. Nicolis
Center for Nonlinear Phenomena and Complex Systems, Université Libre de Bruxelles, Code Postal 231, Boulevard du Triomphe, 1050 Brussels, Belgium

(Received 23 August 2002; revised manuscript received 19 December 2002; published 21 April 2003)

The response of a bistable dynamical system to a deterministic forcing is studied with emphasis on the kinetics of the passage across the barrier separating the two states, and compared to classical Kramers' theory describing the response to a Gaussian white noise forcing. The existence of nontrivial thresholds for the occurrence of transitions is established. Analytic results complemented by numerical simulations are derived for the characteristics of these transitions for periodic and chaotic forcings. The probabilistic properties of the response are finally addressed and some connections are established with the universal stable distributions of probability theory.

DOI: 10.1103/PhysRevE.67.046211 PACS number(s): 05.45.−a, 05.10.Gg

I. INTRODUCTION

Transitions across a barrier separating simultaneously stable states are among the most typical manifestations of nonlinearity. They can be induced by two types of mechanisms.

(i) Initial perturbations exceeding some threshold, bringing the system to the attraction basin of a state other than the unperturbed ''reference'' state.

(ii) External forcings. The most familiar and best studied example of this mechanism is provided by noise-driven systems. In systems whose evolution derives from a potential U the problem can be mapped, following Kramers' pioneering work [1], onto a Langevin equation or, in the presence of Gaussian white noise, onto a diffusion process governed by a Fokker-Planck equation. In the simplest setting of a single variable z, these equations read

$$\frac{dz}{dt} = -\frac{\partial U(z)}{\partial z} + F(t), \tag{1a}$$

$$\langle F(t)\rangle = 0, \quad \langle F(t)F(t')\rangle = q^2\delta(t-t')$$

$$(\text{Langevin equation}) \tag{1b}$$

and

$$\frac{\partial p}{\partial t} = \frac{-\partial}{\partial z}\left(-\frac{\partial U}{\partial z}\right)p + \frac{q^2}{2}\frac{\partial^2 p}{\partial z^2} \quad (\text{Fokker-Planck equation}). \tag{2}$$

Let the noise strength q^2 be much smaller than the *potential barrier* $\Delta U = U(z_0) - U(z_s)$, where z_s and z_0 stand, respectively, for the reference stable state and for the unstable state separating z_s from a second simultaneously stable state. One can then show that the transitions across z_0 depleting the attraction basin of z_s occur on a characteristic time scale given by the Kramers' formula [1]

$$\langle \tau \rangle \approx \pi[-U''(z_0)U''(z_s)]^{-1/2}\exp\left[\frac{2}{q^2}\Delta U\right]. \tag{3}$$

These transitions require no critical threshold: they can be switched on by any nonvanishing value of q^2, however small.

Traditionally noise processes model the effect of heat baths, that is to say, macroscopic systems at fixed temperature composed of many particles such that their state is not affected by the action of the ''small system'' (here described by the variable z) with which they are interacting through some microscopic potential. Such systems are believed to exhibit dynamical chaos at the microscopic level [2]. In this respect, noise and high-dimensional deterministic chaos would appear to be two facets of the same reality.

On the other hand, progress in nonlinear dynamics and, especially, chaos theory leads one to realize that in many situations of interest the coupling of a system to its environment may exclusively involve macroscopic observables undergoing *low-dimensional* nontrivial dynamics. A classical example is provided by the dynamics of a chemically reactive system in a medium undergoing hydrodynamic flow. On a larger scale one may quote the turbulent transport of a minor atmospheric constituent in the atmosphere. In both cases the back action on the environment can be neglected, since the size of the system of interest is much less than that of the environment.

Under the above conditions the external forcing affecting the system's intrinsic dynamics can no longer be assimilated to a noise process. Still the question, can a forcing of this kind induce transitions across the barrier, keeps its full interest. The objective of the present paper is to address this question for a generic class of dynamical systems, with emphasis on the features brought by the deterministic character of the forcing with respect to Kramers' theory, Eqs. (1)–(3). As one could expect, the existence of nontrivial thresholds for the occurrence of transitions is one of these features. We will see how it comes about and how it can be characterized quantitatively. A number of further features will also be iden-

tified, finding their origin in the fact that the probability densities associated to low-dimensional deterministic dynamical systems are defined on finite supports.

The general formulation is developed in Sec. II. Sections III and IV deal, respectively, with the cases of periodic and chaotic forcings. The conditions for the existence of transitions across the barrier are established. Analytic results are derived on the characteristics of the transitions, compared with and complemented by numerical simulations. Section V is devoted to the probabilistic properties of the response, with emphasis on the connections between the probability densities obtained by our analysis and the universal stable distributions of probability theory. The main conclusions are summarized in Sec. VI.

II. GENERAL FORMULATION

Throughout this work we consider systems which, in the absence of forcing, admit two simultaneously stable steady states arising through a supercritical pitchfork bifurcation. The amplitude of the deterministic forcing function relative to the distance from the pitchfork bifurcation will be tuned through a parameter ε. Using the normal form of the supercritical pitchfork bifurcation [3], one may thus write the following evolution equation replacing Eq. (1):

$$\frac{dz}{dt}=\lambda z-z^3+\varepsilon x(t), \tag{4}$$

where $x(t)$ is one of the output variables of an (low-dimensional) ergodic deterministic dynamical system assumed for simplicity to be of zero mean, $\langle x\rangle=0$. Some specific examples considered in Secs. III and IV include the harmonic oscillator, uniform quasiperiodic motion on a torus, the Lorenz equations, or the periodically forced Duffing oscillator. In this setting, the steady state solutions in the absence of the forcing are

$$\begin{aligned} z_{\pm}&=\pm\lambda^{1/2}\quad \text{(stable)},\\ z_0&=0\quad \text{(unstable)}. \end{aligned} \tag{5}$$

The potential U and the potential barrier ΔU are given by

$$U=-\lambda\frac{z^2}{2}+\frac{z^4}{4}, \tag{6a}$$

$$\Delta U=U(z_0)-U(z_{\pm})=\frac{\lambda^2}{4}. \tag{6b}$$

The effective strength of the forcing will be characterized by a suitably chosen norm, $\varepsilon|x|$. For forcings having nontrivial statistical properties, in order to achieve a meaningful comparison with Kramers' theory we will be led to relate the norm to the forcing variance

$$\varepsilon^2|x|^2=q^2=\varepsilon^2\langle x^2\rangle, \tag{6c}$$

where the brackets denote an average taken over the invariant probability density of x.

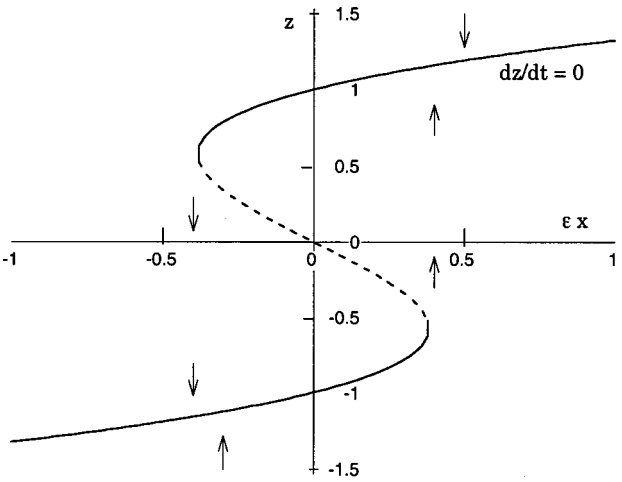

FIG. 1. Hysteretic behavior of the response z versus the forcing εx in the adiabatic limit of Eq. (4) with $\lambda=1$. The arrows indicate the direction of evolution of initial perturbations.

A. The adiabatic limit

To gain a first insight into the behavior of the system just defined, we introduce the scaled variables and parameters

$$\begin{aligned} z&=\lambda^{1/2}w,\\ \varepsilon&=\lambda^{3/2}\eta, \end{aligned} \tag{7}$$

being understood that w, x, and η are of $O(1)$. One obtains

$$\lambda^{-1}\frac{dw}{dt}=w-w^3+\eta x(t). \tag{8}$$

It follows that if λ^{-1} is much smaller than the characteristic time of $x(t)$ the right hand side of Eq. (8) can be set equal to zero. In this *adiabatic approximation*,

$$w^3-w-\eta x=0, \tag{9}$$

the forcing acts as an imperfection perturbing the pitchfork bifurcation. Turning to the initial variables, this leads to a hysteretic behavior of z versus εx, depicted in Fig. 1 (here as well as in the subsequent figures the quantities plotted are dimensionless). Starting, say, from the lower branch at point $(z=-\lambda^{1/2},\varepsilon x=0)$, the system will remain trapped in this branch as long as the forcing has not reached a value corresponding to the right limit point of the *S*-shaped curve. Beyond this threshold the system will rapidly reach the upper branch (in view of the time scale difference referred earlier) and will remain therein until the forcing reaches a second threshold value corresponding to the left limit point, and so on. This leads us to a first estimate of the threshold value of the forcing strength necessary to induce transitions between the two stable states,

$$\varepsilon_c|x|\approx\frac{2}{3\sqrt{3}}\lambda^{3/2}, \tag{10}$$

where the right hand side is obtained by the condition that the discriminant of the cubic equation (9) should vanish in order to have a double real root.

B. Liouvillian dynamics

In order to establish the connection with the white noise limit and Kramers' theory, it is necessary to address the probabilistic properties of the system. The probability density $\rho(z;\varepsilon x)$ for a value z conditioned by a given value of the forcing satisfies the Liouville equation [3]

$$\frac{\partial \rho(z;\varepsilon x)}{\partial t} = -\frac{\partial}{\partial z}[\lambda z - z^3 + \varepsilon x]\rho(z;\varepsilon x). \tag{11}$$

A more relevant quantity is the reduced probability density $q(z)$, obtained by averaging the full ρ over the realizations of the x process (since x is deterministic this implies averaging over an ensemble of initial conditions),

$$q(z,t) = \int dx\, p(z;\varepsilon x)\rho_s(x), \tag{12a}$$

where $\rho_s(x)$ is the invariant probability of x. Since ρ_s is normalized to unity, the passage from ρ to $\overline{q}$ can be viewed as a projection,

$$q = P\rho, \quad P^2 = P. \tag{12b}$$

Introducing the Liouville operator

$$L_t = -\frac{\partial}{\partial z}[\lambda z - z^3 + \varepsilon x(t)] \tag{13}$$

and acting on both sides of Eq. (11) successively by P and $I-P$, one obtains two coupled equations for q and $(I-P)\rho$. Solving formally the second equation with an initial condition in the P space results in a closed equation for q,

$$\frac{\partial q(z,t)}{\partial t} = PLq(z,t) + PL\int_0^t dt'\,\kappa(t,t')(I-P)L_{t'}q(z,t'), \tag{14}$$

where the operator κ is defined by its formal series expansion

$$\kappa = 1 + \int_{t'}^t dt_1 (I-P)L_{t_1} + \int_{t'}^t dt_1 \times \int_{t'}^t dt_2 (I-P)L_{t_1}(I-P)L_{t_2} + \cdots. \tag{15}$$

In this most general form, Eq. (14) is intractable. To obtain some useful information we therefore truncate the infinite series (15) to the first nontrivial (here second) order in ε in the limit of small ε. To allow for transitions between states one should further consider the limit of small λ (vicinity of the pitchfork bifurcation). One obtains then after a straightforward calculation,

$$\frac{\partial q(z,t)}{\partial t} = -\frac{\partial}{\partial z}(\lambda z - z^3)q(z,t) + \varepsilon^2 \frac{\partial^2}{\partial z^2} \times \int_0^t dt'\, C(t-t')q(z,t'), \tag{16a}$$

where $C(t-t')$ is the autocorrelation function of the x process,

$$C(t-t') = \langle x(t)x(t')\rangle. \tag{16b}$$

We stress that truncation to second order alters some of the properties of the exact distribution satisfying the full Eq. (14), in particular, its having a finite support as discussed extensively later in this paper. The motivation for considering this limit is that it allows one to identify a nontrivial difference with the Fokker-Planck equation (2), namely, the non-Markovian character of the dynamics of q. This feature reflects the deterministic origin of the forcing and will also be responsible for some differences of the statistics of transition times as compared to white noise-driven systems as seen in Sec. IV.

One can obtain an indication of the role of memory effects by comparing the contribution of the second term in Eq. (16a) to the contribution of standard diffusion. Performing successively a Fourier and a Laplace transform and applying the convolution theorem, one has

$$[s + \varepsilon^2 k^2 \tilde{C}(s)]\tilde{q}_k = q(0), \tag{17}$$

where k and s are, respectively, the Fourier and Laplace transform variables, the tilde denotes the Laplace transform and $q(0)$ is the initial distribution.

As well known the time-dependent properties of the probability distribution depend on the singularities of its Laplace transform or, equivalently, on the zeros of the factor multiplying $\tilde{q}_k(s)$ in Eq. (17). To fix ideas we consider the following model correlation function:

$$C(t) = e^{-\gamma t}\cos \omega t,$$

$$\tilde{C}(s) = \frac{s+\gamma}{(s+\gamma)^2 + \omega^2},$$

which reproduces the qualitative features of the correlation function of a typical chaotic attractor. The singularities of $\tilde{q}_k(s)$ are then given by

$$s = -\varepsilon^2 k^2 \frac{s+\gamma}{(s+\gamma)^2+\omega^2} \tag{18a}$$

to be compared with those of the Markovian limit obtained by taking $s=0$ in the right hand side of Eq. (18a),

$$s_M = -\varepsilon^2 k^2 \frac{\gamma}{\gamma^2+\omega^2}. \tag{18b}$$

Solving Eq. (18a) iteratively for small s (small k), one obtains

$$s \approx -\varepsilon^2 k^2 \frac{\gamma + s_M}{(\gamma + s_M)^2 + \omega^2} \approx s_M + s_M^2 \frac{\omega^2 - \gamma^2}{\gamma(\gamma^2 + \omega^2)}. \quad (19)$$

Since s_M is negative, s will be smaller in absolute value than $|s_M|$ as long as $\omega > \gamma$ or, equivalently, as long as the decay time of the correlation is not smaller than the period of the background oscillation. This condition is expected to be satisfied in systems generating deterministic chaos organized around an unstable periodic or a homoclinic orbit. Under these conditions the spectrum of characteristic times of diffusion will be shifted toward larger values. We have here identified a second signature of the deterministic character of the forcing: whenever transitions are possible (which according to Sec. II A can happen only when a certain threshold condition is satisfied), they are expected to occur on a time scale longer than the one provided by Kramers' equation (3).

In the sequel, the analysis of this section will be applied to systems subjected to periodic and to chaotic forcings.

III. PERIODIC FORCING

We first consider a purely harmonic forcing. Equation (4) becomes

$$\frac{dz}{dt} = \lambda z - z^3 + a \cos \omega t. \quad (20)$$

Under the scaling of Eq. (7) the adiabatic limit is readily achieved by taking $\omega \ll \lambda$. Owing to the absence of intrinsic variability the natural norm in the threshold condition of Eq. (10) is the maximum norm—the forcing amplitude. This yields

$$a_c = \frac{2}{3\sqrt{3}} \lambda^{3/2}. \quad (21)$$

The numerical integration of Eq. (20) confirms fully this condition. Figure 2(a) depicts the response z in the case of $\omega = 0.1$, $\lambda = 2$ and a value well above the threshold. As can be seen the variable performs transitions between the basins of attraction of the stable states $\pm \lambda^{1/2}$ of the unforced system, with a periodicity equal to that of the forcing. The response is markedly nonsinusoidal, owing to the nonlinearity of the intrinsic dynamics of z. An alternative representation in the form of a bifurcation diagram is provided in Fig. 2(b), where the amplitude of the response is plotted against a. We observe a sharp transition between a small amplitude oscillation around state $\pm \lambda^{1/2}$ and a large amplitude one around zero associated to transitions between the two stable states, at a critical value which is numerically indistinguishable from Eq. (21).

A more intricate situation relates to the presence of multiperiodic or quasiperiodic forcing. To fix ideas, consider a forcing deriving from a uniform quasiperiodic motion. Equation (4) becomes

$$\frac{dz}{dt} = \lambda z - z^3 + \frac{a}{\sqrt{2}} (\cos \omega_1 t + \cos \omega_2 t). \quad (22a)$$

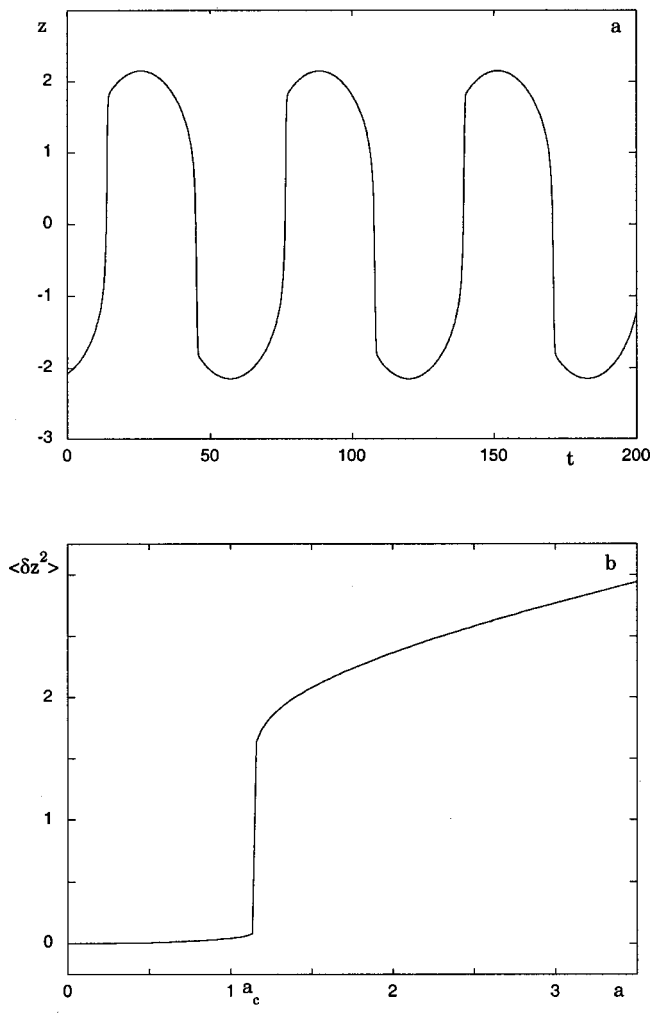

FIG. 2. (a) Long time evolution of z in the presence of a purely harmonic forcing, Eq. (20), with an amplitude well above threshold (21) as provided by the adiabatic approximation. Parameter values are $\lambda = 2$, $\omega = 0.1$, and $a = 2\lambda^{3/2} > a_c$. (b) Bifurcation diagram describing the birth of a large amplitude oscillation of the type depicted in (a) beyond the critical value of the forcing amplitude [Eq. (21)].

The maximum norm and the standard deviation of the forcing are, respectively,

$$|x|_{\max} = \sqrt{2} a, \quad q = \frac{a}{\sqrt{2}}. \quad (22b)$$

We choose $\omega_1 \ll \lambda$ and vary ω_2 gradually from values close to ω_1 to values comparable to or greater than λ. In all cases, a transition from a small amplitude oscillation around one of the stable states $\pm \lambda^{1/2}$ to a large amplitude oscillation around zero is observed as seen in Fig. 3(a). The corresponding critical amplitudes a_c vary according to the relationship between ω_2 and λ, see Fig. 3(b). For ω_2 significantly smaller than λ, a_c is obtained when the maximum norm is used in Eq. (10),

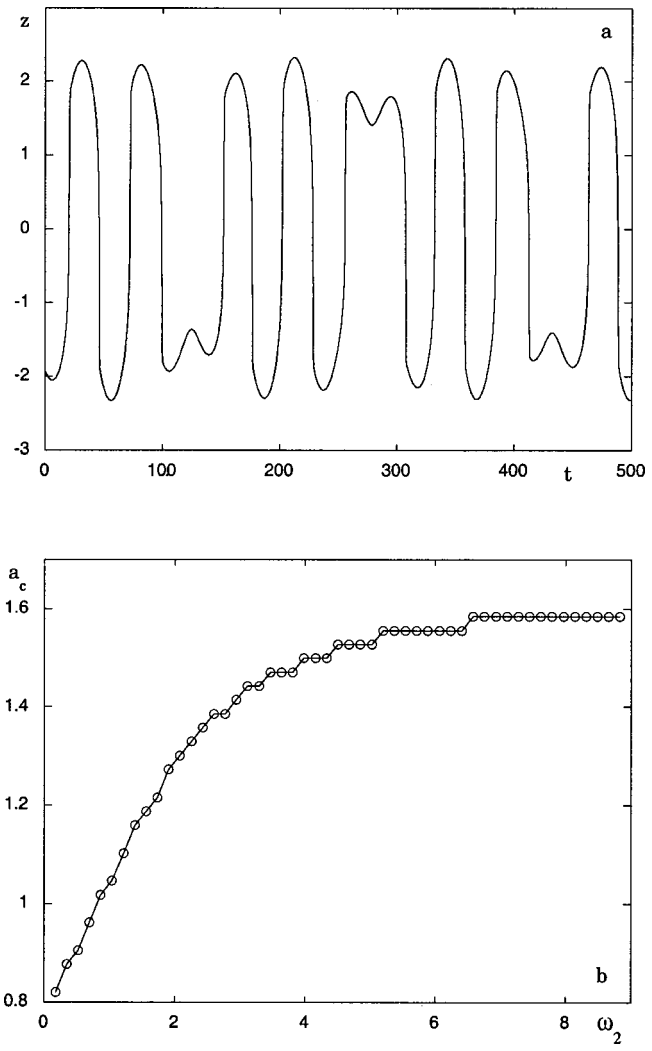

FIG. 3. (a) As in Fig. 2(a) but in the presence of a quasiperiodic forcing with $\omega_1=0.1$, $a=2\lambda^{3/2}$, $\omega_2=\sqrt{2}\omega_1$. (b) Dependence of the critical forcing amplitude a_c necessary for the birth of a large amplitude quasiperiodic oscillation on frequency ω_2 keeping ω_1 and λ at the same values as in (a).

$$a_c=\frac{\sqrt{2}}{3\sqrt{3}}\lambda^{3/2} \quad (\omega_2 \ll \lambda).$$

In contrast, as ω_2 becomes significantly larger than λ the threshold condition (10) is to be formulated in terms of the variance, yielding

$$a_c=\frac{2\sqrt{2}}{3\sqrt{3}}\lambda^{3/2} \quad (\omega_2 \gg \lambda).$$

This result has a straightforward explanation. When all forcing modes are much slower that the system's characteristic times, the adiabatic approximation holds globally. A transition will therefore take place as soon as the maximum value of the forcing will exceed the threshold of Eq. (10). When on the contrary the time scales of the forcing and of the system mix, the adiabatic approximation holds only for the slow modes. The fast modes are ineffective in causing a transition, and this increases the value of the critical amplitude needed to overcome the threshold. The variance provides, then, a more adequate measure of the effective strength. This will be confirmed further in Sec. IV devoted to the effects of a chaotic forcing.

In the remaining part of this section we will be interested in the solutions of Eq. (20) in the vicinity of the bifurcation point and in the limit of weak forcing amplitude. This will allow us to achieve a quantitative understanding of some key aspects of the dynamics of the transitions.

A. The inner expansion

To allow for transitions between states in the above limit one must make sure that the forcing amplitude competes with the distance from the bifurcation. This brings us in the domain of singular perturbation analysis and, in particular, of the inner expansion [4]. Specifically, we adopt the following scaling in Eq. (20):

$$a=\varepsilon b, \qquad \lambda=\varepsilon^2\nu, \quad \varepsilon \ll 1 \tag{23}$$

along with an expansion of z in powers of ε,

$$z=\varepsilon z_1+\varepsilon^2 z_2+\varepsilon^3 z_3+\cdots. \tag{24}$$

To the first few orders, Eq. (20) becomes

$$\frac{dz_1}{dt}=b\cos\omega t, \tag{24a}$$

$$\frac{dz_2}{dt}=0, \tag{24b}$$

$$\frac{dz_3}{dt}=\nu z_1-z_1^3. \tag{24c}$$

Equation (24a) can be integrated straightforwardly to yield

$$z_1=\frac{b}{\omega}\sin\omega t+C. \tag{25}$$

The integration constant C, which also provides the time average of the dominant part z_1 of the solution, is determined from the solvability condition of Eq. (24c). In the present case this condition merely requires that the time average of the right hand side vanishes. Utilizing the fact that the time averages of both $\sin\omega t$ and $\sin^3\omega t$ vanish, one obtains after a straightforward calculation the following algebraic equation for C,

$$\left(\nu-\frac{3b^2}{2\omega^2}\right)C-C^3=0. \tag{26}$$

Equation (26) admits three solutions,

$$C_0=0, \tag{27a}$$

$$C_{\pm} = \pm \left(\nu - \frac{3b^2}{2\omega^2} \right)^{1/2}. \tag{27b}$$

The latter bifurcate from the trivial solution at a value $\nu_c = 3b^2/2\omega^2$ or, reestablishing the original parameters, $\lambda_c = 3a^2/2\omega^2$. Remembering that in the absence of forcing one has $\lambda_c = 0$ and bifurcating branches equal to $z \approx \varepsilon z_1 = \pm \varepsilon \nu^{1/2}$ one deduces that the presence of the forcing preserves the character of the unperturbed pitchfork bifurcation, but shifts the bifurcation point to the right. Now, in the regime of transitions between states one must clearly have a vanishing long time average of z. This means that the solution $C_0 = 0$ should prevail or, alternatively, that $C_{\pm}$ are not real quantities. This can be achieved either by a sufficiently large amplitude b, or by a sufficiently low frequency ω. The latter condition leads us to the adiabatic approximation analyzed earlier in this section, while the former condition yields

$$b > b_c = \sqrt{\frac{2}{3}}\, \omega \nu^{1/2}$$

or, reestablishing the original parameters,

$$a > a_c = \sqrt{\frac{2}{3}}\, \omega \lambda^{1/2}. \tag{28}$$

This relation replaces the threshold condition (21) obtained in the adiabatic approximation, to systems which operate near bifurcation and do not exhibit the time scale separation required by this approximation. Finally, when $a < a_c$ the system performs asymptotically oscillations around a mean value given by C_- or C_+, depending on the initial condition.

The above results are fully corroborated by the numerical integration of Eq. (20) under the conditions of Eq. (23). Figures 4(a,b) describe the time dependence of z obtained when the forcing amplitude is, respectively, larger and smaller than the threshold value a_c. The corresponding bifurcation diagram is depicted in Fig. 4(c). As it turns out the threshold value (28) is reproduced with high accuracy.

From the outset, the analysis performed in this section had been limited to the long time behavior of the solutions. On the other hand, as Fig. 4(b) shows, the basins of attraction of C_+ and C_- are not entirely limited to, respectively, positive and negative z's. This implies that the dynamics should involve nontrivial transient behavior such as an initial condition in the range $z(0) < 0$ evolving toward a stable oscillation around C_+ and, conversely, an initial condition in the range $z(0) > 0$ toward a stable oscillation around C_-. In both cases one would witness an escape over the barrier. This problem is addressed in the following section.

B. Transient behavior: escape over the barrier

The most favorable situation for crossing the barrier in the subcritical case $a < a_c$ is to start near the unstable state $z = 0$ of the unforced system. Equation (20) can then be limited to its linear part,

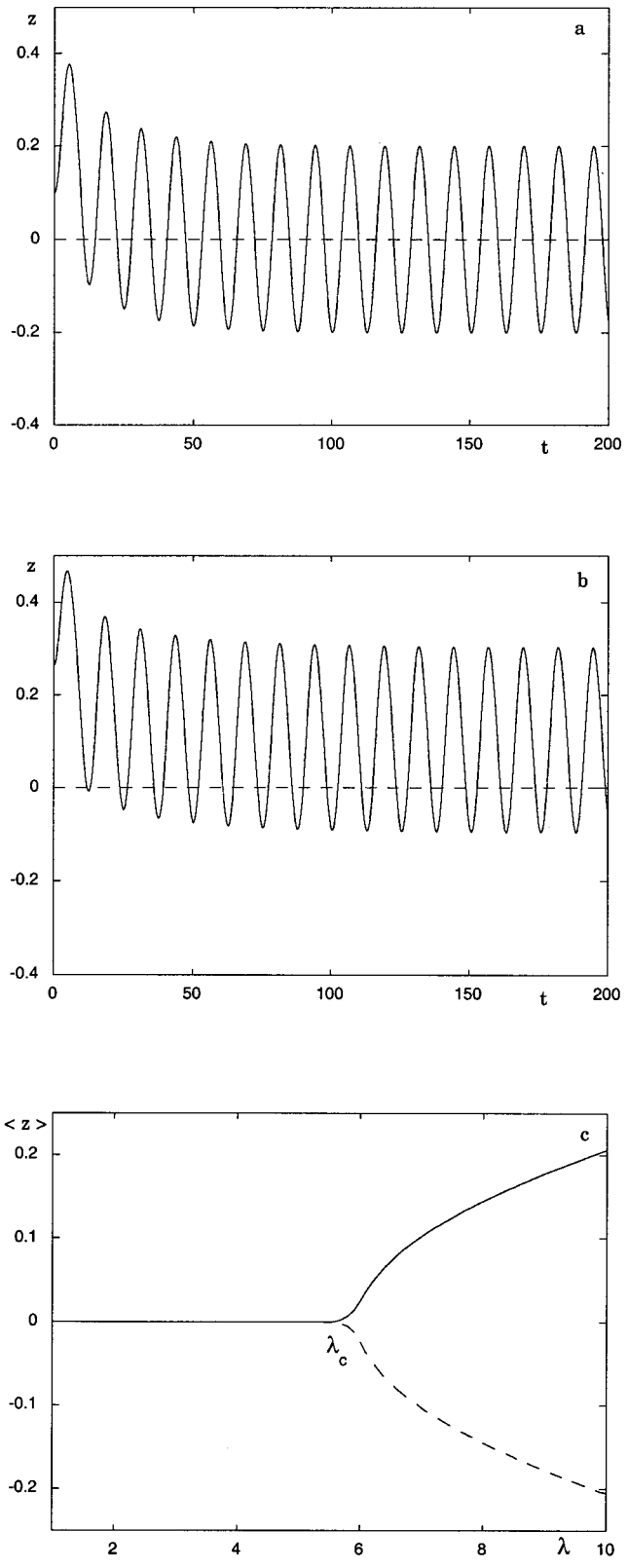

FIG. 4. As in Fig. 2 but when Eq. (20) operates near the bifurcation with a forcing amplitude above threshold (28) and $\lambda = 0.01$ (a) and below threshold (28) and $\lambda = 0.07$ (b). Parameter values are $\omega = 0.5$ and $a = 0.1$.

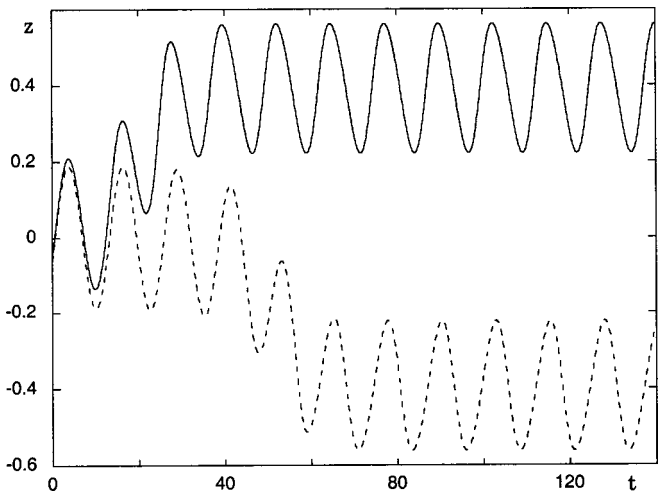

FIG. 5. Transient behavior of z under the conditions of Fig. 4(b) starting from $z(0)=-0.05$ (full line) and $z(0)=-0.062$ (dashed line) with parameter values $\lambda=0.2$, $a=0.1$, and $\omega=0.5$.

$$\frac{dz}{dt}=\lambda z+a\cos\omega t, \tag{29a}$$

whose solution is given by

$$z=z(0)e^{\lambda t}+a\frac{\lambda e^{\lambda t}-\lambda\cos\omega t+\omega\sin\omega t}{\lambda^2+\omega^2}. \tag{29b}$$

It is understood that the system still operates in the range of the scaling of Eq. (23).

We assume (without loss of generality) that $z(0)<0$. We stipulate, in agreement with the numerical solution of the full Eq. (20), that the escape over the barrier and the stabilization to a stable oscillation around C_+ will occur when $z((n+1)T)-z(nT)$ will be positive for $n=0,1,...$, where $T=2\pi/\omega$ is the forcing period (Fig. 5). Using Eq. (29b) we can write this inequality for $n=0$ in the explicit form

$$z(0)>z_c=-\frac{a\lambda}{\lambda^2+\omega^2}. \tag{30}$$

We see that the range of initial conditions escaping from $z<0$ is enhanced as ω and λ are decreased. These rather intuitive conclusions are fully corroborated by the construction of ''state diagrams'' from the numerical solution of the full Eq. (20).

The above analysis can be extended to include the dependence on the phase of the forcing, by solving Eq. (29a) with a forcing term $a\cos(\omega t+\theta)$. The analytic and numerical results are summarized in Fig. 6. Notice the enhanced destabilization for negative forcing phases. This can be understood qualitatively by observing that with such phases the forcing keeps a positive value until the response reaches a second maximum larger than the first one, thereby allowing the system to attain a ''point of no return'' beyond which escape is inevitable.

We next provide estimates of the time necessary to cross the barrier starting from a certain $z(0)$, under the escape

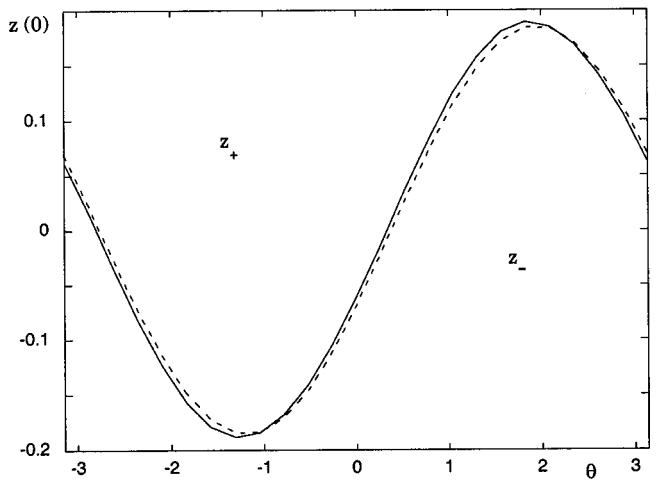

FIG. 6. Range of initial conditions $z(0)$ escaping eventually to the solution of positive mean value z_+ and of negative mean value z_- versus the phase θ of the periodic forcing of Eq. (20) operating near bifurcation under the conditions of Fig. 4(b). Full line represents the numerical results after a transient time of $50\times 2\pi/\omega$ and dashed line stands for the linearized estimate Eq. (30). Parameter values are $\lambda=0.2$, $\omega=0.5$, and $a=0.1$.

condition of Eq. (30). To this end we derive an evolution equation for the excess variable $u(t)=z(t+T)-z(t)$ introduced above, see Ref. [5]. From Eq. (20) one obtains straightforwardly, utilizing the periodicity of the forcing,

$$\frac{du}{dt}=(\lambda-3z^2)u-3zu^2-u^3.$$

In the linearized analysis adopted in this section, one only needs to retain the first term in the right hand side, yielding

$$u(t)=u(0)\exp\left[\lambda t-3\int_0^t dt'\,z^2(t')\right]. \tag{31}$$

For consistency $u(0)\equiv z(T)-z(0)$ is to be evaluated from Eq. (29b), and $z^2(t')$ in the integral is to be replaced by its initial value. The time needed to reach a finite level of $u(t)$, say Δ, can now be estimated by inverting Eq. (31),

$$\tau\approx\frac{1}{\lambda-3z^2(0)}\ln\frac{\Delta}{[z(0)-z_c](e^{\lambda T}-1)}, \tag{32}$$

where z_c is given by Eq. (30). Using a uniform ensemble of initial conditions in the range $(z_c,0)$ one can express the mean crossing time $\langle\tau\rangle$ as

$$\langle\tau\rangle=\frac{1}{|z_c|}\int_{z_c}^{0}dz(0)\,\frac{1}{\lambda-3z^2(0)}\ln\frac{\Delta}{[z(0)-z_c](e^{\lambda T}-1)}$$

or, for $|z_c|\to 0$

$$\langle\tau\rangle\approx\frac{1}{\lambda-3z_c^2}\ln\frac{1}{|z_c|}. \tag{33}$$

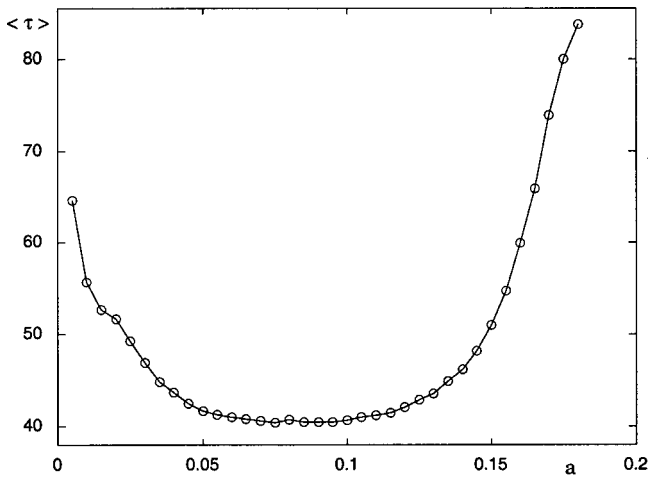

FIG. 7. Time needed in the mean to reach eventually solution z_+ starting from negative z versus the amplitude a of the periodic forcing under the conditions of Fig. 6 with $\theta=0$. Initial conditions scan 2000 values $0 \leqslant z(0) \leqslant -1$.

This expression predicts a logarithmic increase of $\langle \tau \rangle$ with the forcing amplitude—the analog of the parameter q in Kramers' formula (3)—for small forcings, followed by a minimum at a value of a of the order of $\lambda^{1/2}$. This result may be qualified as a stochastic resonancelike effect in the sense that there is an optimal forcing strength for which transitions are facilitated. Alternatively, one may also speak of resonant activation in the sense of Ref. [1] The point is that this type of behavior is quite different from the behavior predicted by Kramers' theory. It is also fully corroborated by numerical solutions of the full equation as shown in Fig. 7.

IV. CHAOTIC FORCING

In this section we deal with the case where the forcing $x(t)$ in Eq. (4) is one of the output variables of a continuous-time chaotic dynamical system. To set the stage we depict in Fig. 8 the time dependence of the response $z(t)$ to a forcing

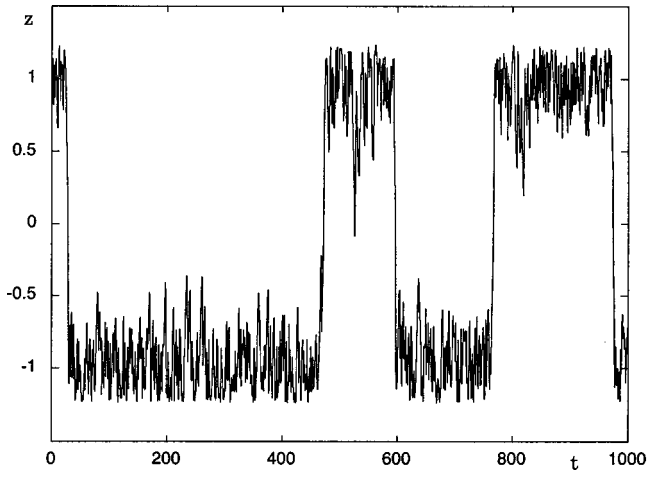

FIG. 8. Long time evolution of z, Eq. (4) sampled every 1 time unit, when the forcing is provided by variable x of the Lorenz system with $r=28$, $\sigma=10$, and $b=\frac{8}{3}$, and for $\lambda=1$, $\varepsilon=0.07$.

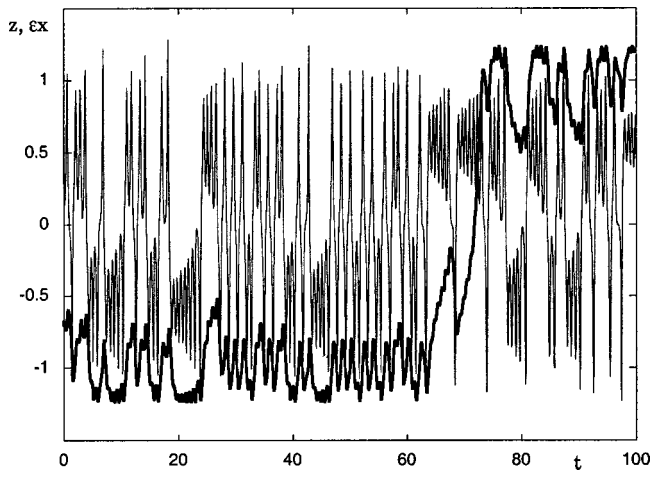

FIG. 9. Kinetics of a transition of z from state z_- to z_+ (dark line) superimposed to the chaotic evolution of the forcing with the same parameter values as in Fig. 8.

$x(t)$ corresponding to the x variable of Lorenz's classic chaotic attractor ($r=28$, $\sigma=10$, $b=\frac{8}{3}$, Ref. [6]) and to a coupling parameter $\varepsilon=0.07$. We see that the variable performs transitions between the attraction basins of the two stable states of the unforced system. To gain a first understanding of the mechanism of these transitions we refer once again to the adiabatic limit (Fig. 1). For the parameter values of Fig. 8, the estimate of Eq. (10) would give a threshold value for the transitions to be switched on of $q_c=0.385$. The numerical solution of Eq. (4) yields the slightly larger value of 0.406 for a waiting time interval 10^5 time units. The difference is acceptable, in view of the fact that $x(t)$ involves a multitude of time scales as a result of which the adiabatic limit cannot be defined as sharply as in the periodic case.

To understand the kinetics of the transitions we consider, in Fig. 9, a zoomed slice of the time series of Fig. 8 along with the time variation of the forcing. As can be seen, the transition (here from negative to positive values of z) requires *repeated* crossings of the threshold q_c by the forcing during a time interval much longer than λ^{-1} throughout which, in addition, the forcing remains positive. The need for such a build up reflects the nontrivial intrinsic variability of the forcing and the inertia of the underlying system—in turn, a consequence of its deterministic character. Similar results are derived (not shown here), in the presence of forcings corresponding to the x variable of the Lorenz's attractor in the range of intermittent behavior [7], or to the position variable of the periodically forced Duffing oscillator [8]. Notice that in the presence of intermittency the threshold estimate of Eq. (10) vastly underestimates the actual value. This reflects the failure of the adiabatic approximation in this case, a fact that can be attributed to the long range correlations characteristic of the intermittent regime.

An interesting view of the response of the system to the chaotic forcing is provided by Fig. 10, where the time cross correlation $\langle x(t)z(t') \rangle$ of the variables x and z (full line) is depicted. We see that the characteristic decay time is very large, much larger than the correlation time of the forcing and the relaxation time of the unforced system. For compari-

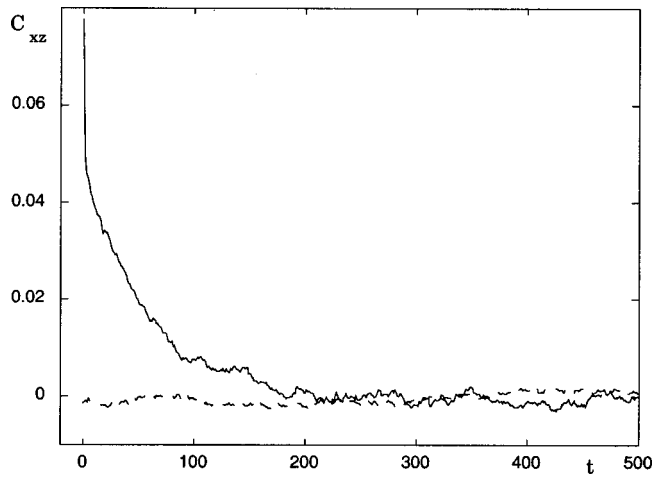

FIG. 10. Cross correlation of the variable $z(t)$ and forcing $\varepsilon x(t)$ under the conditions of Fig. 9 (full line) and the ones provided when $\varepsilon x(t)$ is a Gaussian white noise with variance $q^2=0.15$ (dashed line) such that mean residence times in the attraction basin of the stable states are equal in both systems.

son we also plot (broken line) the cross correlation for a white noise forcing giving rise to the same mean transition time. Long time memory effects have now completely disappeared. These results add credence to the interpretation of the results of Fig. 9 advanced above.

We turn now to a more quantitative analysis of the transitions depicted in Figs. 8 and 9. Figure 11 (empty circles) describes the dependence of the number N of transitions detected in a given (long) time interval for the same type of forcing as in Figs. 8 and 9, as a function of the variance $q^2=\varepsilon^2\langle \delta x^2\rangle$ introduced in Sec. II. As expected, N tends to zero for q below some value—the threshold value identified earlier in this section. Furthermore, the slope of $\ln N$ versus q^2 appears to be very abrupt near this threshold. This is reminiscent of the critical slowing down near the limit point bifurcation associated to q_c (Fig. 1) and suggests a dependence

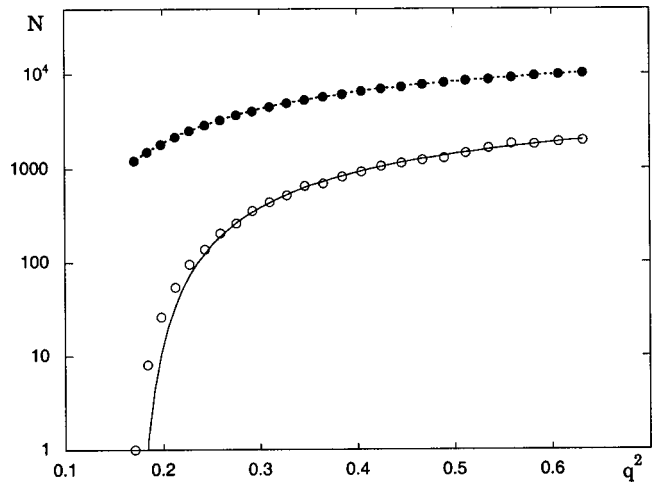

FIG. 11. Number of transitions during 10^5 time units versus q^2 for the system of Fig. 8 (empty circles) and the one corresponding to Kramers' theory (full circles). Full line stands for the best fit by Eq. (34) with $\Delta=1.3247$, $q_c=0.406$, and $N_o=13\,969$.

of $\ln N$ in $(q^2-q_c^2)^{-1/2}$, see Ref. [9]. The full line in Fig. 11 gives a fitting of the numerical data by a function of the form

$$N=N_0\exp\left[\frac{-\Delta}{(q^2-q_c^2)^{1/2}}\right]. \tag{34}$$

The agreement is quite satisfactory, thereby corroborating the arguments just advanced. The exponent Δ featured in Eq. (34) can be interpreted as an effective, forcing-modified "potential barrier" and the prefactor N_0 is proportional to the time interval considered and inversely proportional to the intrinsic time scale of the unforced system.

The upper part in Fig. 11 (full circles) describes the behavior of N as deduced from Eq. (4) subjected to a white noise forcing of variance equal to $\varepsilon^2\langle \delta x^2\rangle$. We are therefore here in the domain of validity of Kramers' theory [N being inversely proportional to $\langle\tau\rangle$, Eq. (3)]. Two major differences with the chaotic forcing-induced transitions are apparent. First, as pointed out already, there is now no threshold value of q: transitions are switched on as soon as q^2 is not zero. And second, for any given values of q^2 above q_c^2 transitions are more frequent in the presence of white noise. This reflects the effect of correlations present in the deterministic forcing. It is also in accord with results where white noise forcing is replaced by a colored noise one, as reviewed in Ref. [1]. Notice that the range of validity of Kramers' theory is actually restricted to values of q^2 less than or about equal to q_c^2, since for the values considered in Fig. 11 the potential barrier ΔU is equal to 0.25.

Similar results (not shown here) are derived for a forcing $x(t)$ given by Lorenz's equations in the intermittent region [7] and by the periodically forced Duffing oscillator [8]. The main differences are as follows. In the first case, as mentioned earlier, the threshold q_c is much higher. The fitting with Eq. (34) is also less satisfactory, owing presumably to the fact that the adiabatic limit and hence the relevance of the limit point bifurcation (Fig. 1) are not applicable. As for the second case, one observes a plateau region of $\ln N$ for intermediate values of q. We conjecture that this reflects the bimodal character of the probability density associated to x, entailing that the variance is no longer as representative as in the monomodal case corresponding to Fig. 11.

The results pertaining to Fig. 11 can also be expressed in terms of the transition times themselves. We first recall that as it was already remarked, the mean transition times are inversely proportional to the quantity plotted in Fig. 11. A more comprehensive information is provided by the probability density of the transition times. In white noise-driven bistable systems this distribution is exponential in the Kramers' regime [10],

$$P(\tau)=\langle\tau\rangle^{-1}\exp(-\tau/\langle\tau\rangle) \quad \text{(white noise-driven system)}. \tag{35}$$

Figure 12 summarizes the differences arising when the bistable system is driven by a chaotic forcing. Here the probability densities are plotted for two different values of the variance, curves (a) and (b). We observe a difference of the densities associated to chaotic forcings (full lines) from the

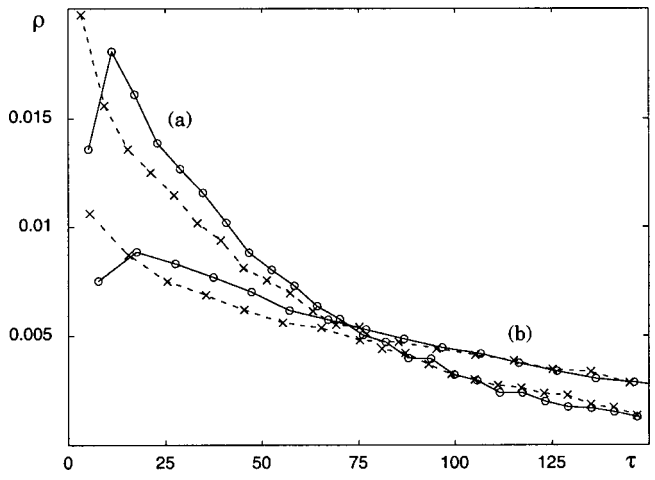

FIG. 12. Probability densities of transition times when the system is driven by the x variable of the Lorenz system of variance $q^2=0.40$ (a) and $q^2=0.31$ (b) (full lines); and by a Gaussian white noise (dotted lines) leading to the same mean value $\langle\tau\rangle$ as the deterministic forcing as obtained from 50 000 transitions. The associated forcing variances in this latter case are $q^2=0.20$ and $q^2=0.15$, respectively.

law of Eq. (35) in the form of a depression for small τ's followed by an overshoot and, finally, by a rapid exponential-like decrease. We suggest that the origin of this behavior is in the non-Markovian character of the truncated Liouvillian dynamics (Sec. II B), entailing that transitions in the range of short times are penalized. We have also plotted in the same figure the probability densities of transition times corresponding to a white noise (dashed lines). To render the comparison meaningful, we consider distributions having the same mean transition times [$\langle\tau\rangle\sim 55$ (a); $\langle\tau\rangle\sim 120$ (b)] as those generated by the chaotic forcing (meaning that the associated variance values are different). While in the white noise-driven system the exponential of Eq. (35) provides a perfect fit, the distribution in the chaotically driven system is significantly different for times up to values of the order of the mean value $\langle\tau\rangle$.

We finally address the effect of a weak chaotic forcing acting in the vicinity of the pitchfork bifurcation of the unforced system. The main point is that in the range of the scaling of Eq. (23) the expansion of Eq. (24) becomes inadequate. Specifically, it leads to the dominant order to the equation

$$\frac{dz_1}{dt}=x(t), \tag{36}$$

which defines a *nonstationary* process z as long as $x(t)$ is a stationary process with a finite correlation time, as is the case of typical chaotic systems contrary to periodic ones (see Sec. V for a more detailed discussion of this point). To get some insight on the response we therefore adopt the more traditional outer expansion [5] in which z in Eq. (4) is expanded as

$$z=\pm\lambda^{1/2}+\varepsilon z_1+\varepsilon^2 z_2+\cdots, \tag{37}$$

keeping first the parameter λ to $O(1)$. Taking, to fix ideas, the plus sign in Eq. (37) one obtains to the first few orders

$$\frac{dz_1}{dt}=-2\lambda z_1+x(t), \tag{38a}$$

$$\frac{dz_2}{dt}=-2\lambda z_2-3\lambda^{1/2}z_1^2. \tag{38b}$$

The solution of Eq. (38a) subject to $z_1(0)=0$ is

$$z_1(t)=e^{-2\lambda t}\int_0^t d\tau\, e^{2\lambda\tau}x(\tau) \tag{39}$$

with $\langle z_1\rangle=0$. In contrast z_2 has a nontrivial average value given by

$$\langle z_2\rangle=-\frac{3}{2\lambda^{1/2}}\langle z_1^2\rangle. \tag{40}$$

This contribution can be qualified as ''destabilizing'' in the sense that the gap between the reference state $\lambda^{1/2}$ of the unforced system and the unstable state $z=0$ is reduced. Computing $\langle z_1^2\rangle$ from Eq. (39) one obtains

$$\langle z_1^2\rangle=-\frac{3}{2\lambda^{1/2}}e^{-4\lambda t}\int_0^t d\tau'\int_0^t d\tau''\, e^{2\lambda(\tau'+\tau'')}C_{xx}(\tau'-\tau''), \tag{41}$$

where $C_{xx}(t)$ is the autocorrelation function of the forcing variable x. As an example for an exponentially decaying C_{xx},

$$C_{xx}(t)=C_0e^{-\gamma|t|}, \tag{42}$$

one obtains

$$\langle z_2\rangle=-\frac{3C_0}{2\lambda^{1/2}}\frac{1}{2\lambda(2\lambda+\gamma)}. \tag{43}$$

This provides one with an estimate of the threshold value of ε^2C_0 (the analog of q^2 of our previous analysis) necessary to overcome the unstable point $z=0$,

$$\lambda^{1/2}+\varepsilon^2\langle z_2\rangle_c=0,$$

or

$$(\varepsilon C_0^{1/2})_c\approx\frac{2\lambda}{\sqrt{3}}(2\lambda+\gamma)^{1/2} \tag{44}$$

to be compared with Eq. (29) derived in the case of the periodic forcing. For ε below this value the long time behavior of the system will be a chaotic oscillation around a mean given by $\pm(\lambda^{1/2}+\varepsilon^2\langle z_2\rangle)$; and for ε above this value transitions between the two attraction basins of the unforced system are expected. These predictions are corroborated by the numerical solution of the full equations.

V. PROBABILISTIC STRUCTURE OF THE RESPONSE

In this section we analyze the consequences of the property of $x(t)$ to derive from a probability distribution possessing a *bounded support* as opposed to the infinite support of the normal distribution involved in Gaussian white noise and of other universal distributions of probability theory. The specific question we shall address pertains to the repercussions of this property in the probabilistic structure of the response variable z. Could it be that the probability distribution of z is attracted toward one of the stable laws of probability theory [11] or, rather, does it keep a finite support and if so how is it related to the characteristics of $\rho(x)$. We shall limit our analysis to forcings generated by low-dimensional chaos. High-dimensional chaotic dynamical systems such as spatially extended systems or coupled locally chaotic cells are indeed known to produce, under certain conditions, probability distributions approaching those of stochastic systems [12].

In order to disentangle the relative roles of damping and of nonlinearity we first consider the limiting situations associated to two truncated versions of Eq. (4) before addressing the full problem,

$$\frac{dz}{dt}=\varepsilon x(t), \tag{45}$$

$$\frac{dz}{dt}=-\lambda z+\varepsilon x(t), \tag{46}$$

to which we shall refer, respectively, as the generalized Wiener process and the generalized Ornstein-Uhlenbeck process.

A. The generalized Wiener process, Eq. (45)

Integrating Eq. (45) one has

$$z(t)-z(0)=\varepsilon\int_0^t d\tau\, x(\tau)\approx\varepsilon\Delta t\sum_{j=1}^{N\Delta t}x(j\Delta t). \tag{47}$$

In this representation $z(t)-z(0)$ is expressed as a sum of variables, each term of the sum being distributed according to a density carried by a finite interval (which is the same for all terms in view of ergodicity). On the other hand, keeping in mind that $\langle x\rangle=0$ and hence $\langle z\rangle=0$ as well one obtains for the variance of z,

$$\langle\delta z^2\rangle=\varepsilon^2\int_0^t d\tau\int_0^t d\tau'\langle x(\tau)x(\tau')\rangle$$

$$\approx 2\varepsilon^2\int_0^t d\tau\int_0^\tau d\eta C_{xx}(\eta).$$

As long as $C_{xx}(\eta)$ is short ranged, the upper limit of the second integral can be pushed to infinity and one has

$$\langle\delta z^2\rangle\approx t \tag{48}$$

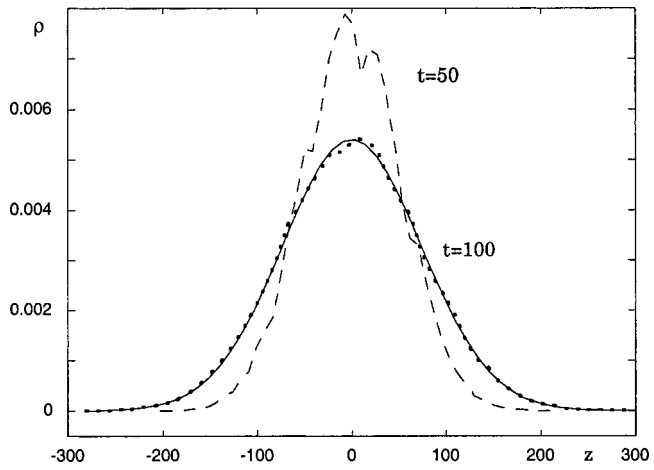

FIG. 13. Probability density of z, Eq. (45), with $x(t)$ the variable x of the Lorenz system after $t=50$ time units (dashed line) and $t=100$ time units (dotted line). Full line is a Gaussian probability density with the same variance.

indicating a diffusive behavior of z. More to the point, the conjunction of Eq. (48), in particular of the fact that $\langle\delta z^2\rangle\to\infty$, and of the finite support of the terms in the sum (47) implies that the Lindeberg condition familiar from probability theory is satisfied [11]. It follows that the distribution of z tends to the normal distribution, one of the stable laws of probability theory and the only for which a second moment exists. The dashed and dotted lines of Fig. 13 depict the density of z at two different times resulting from numerical integration of Eq. (45) and with a forcing x given by the Lorenz x variable, while the full one is a fit by a Gaussian distribution having the same variance. The agreement is very satisfactory. Clearly, we have here a universal mechanism of deterministic diffusion.

B. The generalized Ornstein-Uhlenbeck process, Eq. (46)

The solution of Eq. (46) reads

$$z(t)-z(0)=\varepsilon e^{-\lambda t}\int_0^t d\tau\, e^{\lambda\tau}x(\tau)$$

$$\approx\varepsilon\Delta t\sum_{j=1}^{N\Delta t}e^{-\lambda\Delta t(N-j)}x(j\Delta t) \tag{49}$$

implying that $z(t)-z(0)$ is again a sum of terms each one of which possesses a distribution with a finite support. But in contrast to the case in Sec. V A, the variance of $z(t)-z(0)$ is now

$$\langle\delta z^2\rangle=2\varepsilon^2e^{-2\lambda t}\int_0^t d\tau\, e^{2\lambda\tau}\int_0^\tau d\eta\, e^{-\lambda\eta}C_{xx}(\eta).$$

While, as in Sec. V A, the second integral gives a finite contribution, the divergence found in Sec. V A is now counteracted by the exponentially decaying factor $e^{-2\lambda t}$, entailing that $\langle\delta z^2\rangle$ tends to a finite value as $t\to\infty$. It follows that the Lindeberg condition is not satisfied this time and, since the

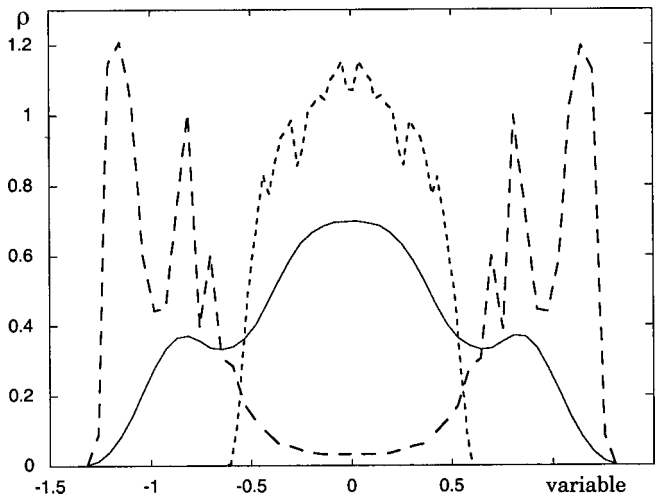

FIG. 14. Probability densities of variable x of the Lorenz system (full line); of z, Eq. (46) (dotted line); and of the full nonlinear system, Eq. (4) (dashed line) with $\lambda=1$ and $\varepsilon=0.07$ as obtained after an integration of 10^6 time units sampled every $\Delta t=0.1$ time units.

distribution of x itself is not Gaussian (contrary to a white noise forcing, see Ref. [13]), the distribution of z will *not* be attracted by the Gaussian distribution [11]. As a matter of fact it will not be attracted by any of the other stable laws since, contrary to these laws, it possesses a second moment. The dotted line in Fig. 14 depicts the asymptotic ($t\to\infty$) distribution of z when Eq. (46) is forced by the Lorenz x variable (the distribution of which is shown in the figure by the full line), as obtained from numerical integration. The distribution possesses now a finite support, contrary to the case of Fig. 13. Although its analytic structure cannot be obtained in closed form it can formally be represented as an infinite convolution along the lines of Ref. [11], Chap. VIII 5. The fine structure persists when the z space is divided into 50 up to ~20 bins, but no convincing explanation can be advanced at this stage.

C. The nonlinear case, Eq. (4)

We turn finally to the full nonlinear problem [Eq. (4)]. For a Gaussian white noise forcing $\varepsilon x(t)$, the probability density of the response z would be a bimodal distribution with two equal maxima located at $z=\pm\lambda^{1/2}$, a minimum at $z=0$ and tails tending exponentially to zero as $|z|\to\infty$. In the presence of a deterministic forcing (here given by the Lorenz x variable) the situation is substantially different, as illustrated by the dashed line of Fig. 14. First, as in the two previous sections, $\rho(z)$ is limited to a finite support. Furthermore, while the absolute minimum at $z=0$ persists, the probability density of the response seems to possess local minima at $z=\pm\lambda^{1/2}$, reflecting the splitting of the probability mass on the two sides of $z=0$ into two secondary peaks situated on the two sides of $\pm\lambda^{1/2}$. This fine structure seems to be statistically stable: it persists when the z space is divided into 50 up to ~25 bins, and disappears (to become a simple bimodal distribution) only in the much coarser subdivision into 14 bins. We suggest that it may find its origin in the local maxima of the probability density of x on the two sides of $x=0$ at x values beyond the threshold value of q_c in Eq. (10) but below $\pm\lambda^{1/2}$. This favors transitions to z values different from $\pm\lambda^{1/2}$ and, since these states have sizable lifetimes owing to the deterministic character of the dynamics, they contribute significantly to the probability mass. This accounts for the inner secondary peaks. As for the outer ones, they may simply reflect the fact that $\rho(z)$ must strictly drop to zero not far from $\pm\lambda^{1/2}$. A similar phenomenon happens in a harmonically forced linear system, whose probability density displays an integrable singularity at the end points of its support.

VI. CONCLUSIONS

In this work some features brought when a dynamical system transits across a barrier under the effect of a deterministic forcing have been identified, as compared to the familiar case of Gaussian white noise-induced transitions. Both the adiabatic limit and the vicinity of bifurcation have been explored for forcings deriving from low-dimensional dynamics such as simple harmonic, periodic nonharmonic, quasiperiodic, and chaotic. It was shown that owing to the finite support of the probability density of the forcing, the occurrence of transitions requires nontrivial threshold conditions. This gives rise to a dependence of the rate of transitions on the forcing strength (variance) which is quite different from the one featured by Kramers' theory. This property in conjunction with the memory effects inherent in the deterministic character of the forcing also entails that when possible, transitions occur on a slower time scale.

The finite support of the forcing probability density has also some repercussions in the probabilistic structure of the response. Typically, the response probability density also possesses a finite support. As a result it has no universal character, contrary to the stable distributions featured in the probability theory. It is only in the limit where the nonlinearity and the damping are absent, referred as the ''generalized Wiener process'' in Sec. V, that one tends to a stable law in the form of the Gaussian distribution, reflecting the onset of deterministic diffusion.

The work reported in this paper can be extended in several ways. For one-variable systems, other types of bifurcation such as the limit point and transcritical bifurcations as well as higher codimension phenomena (butterfly catastrophes, etc.) deserve study. Another interesting class is multivariate systems, since they can possess simultaneously stable steady states, limit cycles and more complex sets, separated by nontrivial invariant manifolds. Finally, a natural question to raise is whether, in this setting, stochastic resonancelike effects could be induced by the presence of a secondary periodic forcing.

ACKNOWLEDGMENTS

The present work was supported, in part, by the Belgian Federal Office for Scientific, Technical and Cultural Affairs under Contract No. MO/34/004 and by the European Space Agency.

[1] For a review, see P. Hänggi, P. Talkner, and M. Borkovec, Rev. Mod. Phys. **82**, 251 (1990).
[2] P. Gaspard, *Chaos, Scattering and Statistical Mechanics* (Cambridge University Press, Cambridge, 1998).
[3] G. Nicolis, *Introduction to Nonlinear Science* (Cambridge University Press, Cambridge, 1995).
[4] S. Rosenblat and D. Cohen, Stud. Appl. Math. **63**, 1 (1980).
[5] M. Gitterman and G. Weiss, J. Stat. Phys. **70**, 107 (1993).
[6] E. Lorenz, J. Atmos. Sci. **20**, 130 (1963).
[7] C. Sparrow, *The Lorenz Equations* (Springer, Berlin, 1982).
[8] J. Guckenheimer and Ph. Holmes, *Nonlinear Oscillations, Dynamical Systems and Bifurcations of Vector Fields* (Springer, Berlin, 1983).
[9] G. Dewel, P. Borckmans, and D. Walgraef, J. Phys. Chem. **88**, 5442 (1984).
[10] C. Gardiner, *Handbook of Stochastic Methods* (Springer, Berlin, 1983).
[11] W. Feller, *An Introduction to Probability Theory and its Applications* (Wiley, New York, 1971), Vol. II.
[12] G. Nicolis, M. Op de Beeck, and C. Nicolis, Physica D **103**, 73 (1997).
[13] J. Doob, Ann. Math. **43**, 351 (1942).